

Title:

Inhibitory Gating Modulation of Small Conductance Ca^{2+} -Activated K^{+} Channels by the Synthetic Compound NS8593 Reduces I_{AHP} in Hippocampal CA1 Neurons*

Authors:

Dorte Strøbæk, Charlotte Hougaard, Tina H. Johansen, Ulrik S. Sørensen, Elsebet Ø. Nielsen, Karin S. Nielsen, Ruth D. T. Taylor, Paola Pedarzani, Palle Christophersen

Addresses:

NeuroSearch A/S, Pederstrupvej 93, DK 2750 Ballerup, Denmark. (D.S., C.H., T.H.J., U.S.S., E.Ø.N, K.S.N., P.C.)

Department of Physiology, University College London, Gower Street, London WC1E 6BT, UK. (R.T., P.P.).

Running title: *Inhibitory Gating Modulation of SK Channels*

Corresponding author:

Palle Christophersen

NeuroSearch A/S, Pederstrupvej 93, DK 2750 Ballerup, Denmark

Tlf: +45 44 60 82 22

Fax: +45 44 60 80 80

E-mail: pc@neurosearch.dk

Text pages: 23

Number of tables: 2

Number of figures: 8

Number of references: 44

Words in Abstract: 246

Words in Introduction: 748

Words in Discussion: 1248

Abbreviations: ACSF, artificial cerebrospinal fluid; BK, large conductance Ca^{2+} -activated K^{+} channel; BMB, bicuculline methobromide; ChTX, charybdotoxin; Clot, clotrimazole; CNS, central nervous system; dTC, d-tubocurarine; 1-EBIO, 1-ethyl-2-benzimidazolinone; eDRG, embryonic dorsal root ganglion; fAHP, fast afterhyperpolarization; HEK, human embryonic kidney; hERG, human ether-a-go-go-related gene; I_{AHP} , afterhyperpolarizing current; I_{C} , Ca^{2+} - and voltage-dependent current; IK, intermediate conductance Ca^{2+} -activated K^{+} channel; NS309, 6,7-dichloro-1H-indole-2,3-dione 3-oxime; NS8593, (R)-N-(benzimidazol-2-yl)-1,2,3,4-tetrahydro-1-naphthylamine; sAHP, slow afterhyperpolarization; sI_{AHP} , slow afterhyperpolarizing current; SK, small conductance Ca^{2+} -activated K^{+} channel; TTX, tetrodotoxin; UCL 1684, 6,10-diaza-3(1,3),8(1,4)-dibenzena-1,5(1,4)-diquinolinacyclodecaphane; XE991, 10,10-bis(4-pyridinylmethyl)-9(10H)-anthracenone dihydrochloride.

ABSTRACT

SK channels are small conductance Ca^{2+} -activated K^+ channels important for the control of neuronal excitability, the fine tuning of firing patterns and for the regulation of synaptic mechanisms. The classical SK channel pharmacology has largely focused on the peptide apamin, which acts extracellularly by a pore blocking mechanism. Recently, 1-EBIO and NS309 have been identified as positive gating modulators that increase the apparent Ca^{2+} -sensitivity of SK channels. In the present study we describe inhibitory gating modulation as a novel principle for selective inhibition of SK channels. In whole-cell patch clamp experiments the compound (*R*)-*N*-(benzimidazol-2-yl)-1,2,3,4-tetrahydro-1-naphthylamine (NS8593) reversibly inhibited recombinant SK3-mediated currents (hSK3 and rSK3) with potencies around 100 nM. However, in contrast to known pore blockers, NS8593 did not inhibit [^{125}I]apamin binding. Using excised patches it was demonstrated that NS8593 decreased the Ca^{2+} -sensitivity by shifting the activation curve for Ca^{2+} to the right, only slightly affecting the maximal Ca^{2+} -activated SK current. NS8593 inhibited all the SK1-3 subtypes Ca^{2+} -dependently ($K_d = 0.42, 0.60, \text{ and } 0.73 \mu\text{M}$, respectively at $0.5 \mu\text{M } \text{Ca}^{2+}$) whereas the compound did not affect the Ca^{2+} -activated K^+ channels of intermediate and large conductance (hIK and hBK channels). The site of action was accessible from both sides of the membrane and the NS8593-mediated inhibition was prevented in the presence of a high concentration of the positive modulator NS309. NS8593 was further tested on mouse CA1 neurons in hippocampal slices and shown to inhibit the apamin- and tubocurarine-sensitive SK-mediated current, I_{AHP} , at a concentration of $3 \mu\text{M}$.

The excitability and the patterns of action potential firing of neurons as well as the function and plasticity of synapses are balanced by the activity of many ion channels, including small conductance Ca^{2+} -activated K^+ channels (SK channels) (Faber et al., 2005; Ngo-Anh et al., 2005). SK channels mediate a Ca^{2+} -activated afterhyperpolarizing current, I_{AHP} , in neocortical, hippocampal and amygdala pyramidal cells, whereas BK channels are responsible for an earlier component of the afterhyperpolarization (fAHP, I_{C}). The channels mediating the long-lasting, Ca^{2+} -dependent afterhyperpolarization (sAHP, sI_{AHP}) in these neurons have not yet been identified (for recent reviews on SK channels, see Stocker, 2004; Bond et al., 2005).

Three SK channel subunits have been cloned (SK1-3), which exhibit distinct, but partly overlapping distributions in the CNS (Kohler et al., 1996; Stocker and Pedarzani, 2000; Sailer et al., 2004). The three subunits are highly homologous and have indistinguishable biophysical properties in terms of single channel conductance, rectification, selectivity and gating, which is governed by Ca^{2+} -binding to calmodulin constitutively attached to the C-terminus of each subunit (Xia et al., 1998). Despite the structural and functional similarities of homomultimeric SK channels, various peptide toxins block the SK1, SK2 and SK3 subtypes with different potencies. The classical blocker of SK channels is apamin, an alkaline 18 amino acid peptide from the venom of the honeybee *Apis mellifera*. Apamin is a pore blocker carrying positively charged amino acids (Arg^{13} and Arg^{14}) as well as a neutral amino acid (Gln^{17}), which are thought to interact with negative (Asp^{341}) and neutral (Asn^{368}) amino acids, positioned in the outer pore mouth of SK channels (Ishii et al., 1997). The interaction is highly potent (affinities in the pM to nM range) and selective with the blocker selectivity sequence: SK2 > SK3 > SK1 (for a review, see Stocker et al. 2004). The IK channel, which is closely related to SK channels, is not blocked by apamin, neither is any other known mammalian K^+ channel. This makes apamin an SK-specific blocker, and it has therefore been extensively used as a reliable and valuable tool for the identification of SK-mediated physiological responses in isolated cells, tissues and, to a lesser extent, in whole animals (for a review,

see Blank et al., 2004). The potent scorpion toxins scyllatoxin (from *Leiurus quinquestriatus*, Chicchi et al., 1988) and the recently described tamapin (from *Mesobuthus tamulus*, Pedarzani et al., 2002), both displace apamin from its binding site and exhibit blocker selectivity similar to apamin. Based on scyllatoxin, an artificial peptide called Lei-Dab⁷, with considerably improved selectivity for SK2 channels, has been synthesized (Shakkottai et al., 2001). Furthermore, a number of lower potency (μM) compounds, such as the anticholinergic d-tubocurarine and dequalinium (Castle et al., 1993), and quaternary methyl derivatives of bicuculline (Seutin and Johnson, 1999), block SK channels and displace apamin from its binding site (Finlayson et al., 2001). Finally, SK channels have been the focus for rational drug design targeting the apamin site. This has resulted in very potent, positively charged, small-molecule blockers with potencies around 1 nM, such as the bis-quinolinium cyclophane UCL 1684 (Campos Rosa et al., 2000, for a review, see Liegeois et al., 2003).

The SK and IK channels can be positively modulated by a number of small heterocyclic organic molecules of which the prototype compound is the benzimidazolinone 1-EBIO (Syme et al., 2000; Pedarzani et al., 2001), and the most potent compound described thus far is the indole-oxime NS309 (Strøbæk et al., 2004; Pedarzani et al., 2005). The positive modulation is due to a concentration-dependent increase in the Ca^{2+} -sensitivity of the SK channels. Mutagenesis studies suggest a binding site for 1-EBIO involving the C-terminal region of the SK channels (Pedarzani et al., 2001). In contrast to the peptide blockers, the positive modulators are slightly more potent on IK channels as compared to the SK channel subtypes.

In the present paper, we describe a new potent and selective inhibitor of recombinant SK channels and of the SK-mediated, apamin-sensitive I_{AHP} in hippocampal CA1 neurons. Thus, as a result of our medicinal chemistry effort we identified the compound (*R*)-*N*-(benzimidazol-2-yl)-1,2,3,4-tetrahydro-1-naphthylamine (NS8593) which is chemically distant from all previously known small-molecule blockers of SK channels and does not carry permanent positive charges (Sørensen et al., 2006). NS8593 acts through a novel mechanism by decreasing the Ca^{2+} -sensitivity of SK channels rather than blocking their

pore. NS8593 is therefore the first inhibitory gating modifier of SK channels described so far. The mechanism of action of NS8593 on SK channels is discussed together with possible implications for drug development.

Materials and Methods

Chemical synthesis of NS8593

NS8593 (**1**) was synthesized in a one-step reaction from commercially available 2-chlorobenzimidazole (**2**) and (*R*)-1,2,3,4-tetrahydro-1-naphtylamine (**3**). Thus, **2** (5.0 g, 32.8 mmol) and **3** (5.8 g, 39.3 mmol) were suspended in acetonitrile (5 ml) in a closed vial and heated to 170°C for 40 minutes by microwave irradiation (Emrys Optimizer EXP, Biotage, Sweden). After cooling the reaction mixture to room temperature, the precipitated solid was filtered off and washed with acetonitrile to give **1** as a hydrochloride salt in 65% yield.

In order to evaluate the enantiomeric purity of **1**, its optical rotation was measured and compared with that of the corresponding (*S*)-enantiomer prepared from **2** and commercially available (*S*)-1,2,3,4-tetrahydro-1-naphtylamine (reacting for six days in refluxing toluene using conventional heating). The optical rotation of the (*S*)-enantiomer and that of **1** were determined at -55.8° and 58.7° (MeOH, 25°C), respectively. In the compound characterization of **1** the following additional data was obtained (for the HCl salt). Melting point 263-265°C; MS(ES⁺) *m/z* 264 ([*M* + 1]⁺, 100%); ¹H NMR (DMSO-d₆) δ 1.75-1.85 (m, 1H), 1.88-1.97 (m, 2H), 2.06-2.13 (m, 1H), 2.72-2.88 (m, 2H), 5.01-5.07 (m, 1H), 7.16-7.28 (m, 5H), 7.34-7.43 (m, 3H), 9.48 (m, 1H), 12.8 (br s, 2H); ¹³C NMR (DMSO-d₆) δ 19.7, 28.8, 30.0, 51.9, 111.7, 123.2, 126.4, 127.9, 128.8, 129.4, 130.4, 135.5, 137.6, 150.0. Elemental analysis (Department of Chemistry, University of Copenhagen): Anal. Calcd. for C₁₇H₁₇N₃•HCl: C, 68.11; H, 6.05; N, 14.02; Found: C, 67.87; H, 5.97; N, 13.98.

Scheme 1

Cell cultures

Apamin binding and patch clamp studies using recombinant channels were performed on HEK293 cells stably expressing the various channels. Establishment of hSK1, rSK2, hSK2, rSK3, hSK3, and hIK channel cell lines was described in (Strøbæk et al., 2004). Selectivity studies were performed on BK channels (see Strøbæk et al., 1996 for cloning and expression), K_v7.2+7.3 channels (Schröder et al., 2001), hERG channels (T. Ljungstrøm, PhD thesis, 2002, University of Copenhagen), rNa_v1.2 channels (M.P.G. Korsgaard, PhD thesis, University of Copenhagen, 2001) as well as native voltage-dependent Na⁺, Ca²⁺ and K⁺ channels in rat embryonic dorsal root ganglion (eDRG) neurons.

Cell lines were cultured in Dulbeccos Modified Eagles Medium (DMEM, BioWittaker, Walkersville, MD, USA) supplemented with 10% fetal calf serum (Sigma-Aldrich, Værløse Strand, Denmark). At 60-80% confluency cells for patch clamp experiments were harvested by trypsin treatment and seeded on cover slips (Ø 3.5 mm, custom made at VWR international APS, Denmark) placed in a petri dish. Cells for apamin binding assays were cultured to 80-90% confluence, the medium was removed and cells were rinsed with 10 ml Phosphate Buffered Saline (PBS) and harvested by scraping. The cell suspension was centrifuged for 10 min (27,000 x g) at 4°C, and the pellet was resuspended by homogenization in 50 mM Tris-HCl (pH 7.4) and centrifuged. The final HEK293/hSK3 pellet was suspended in buffer and stored at -80°C.

[¹²⁵I]Apamin binding

Male Wistar rats (150-200g, Taconic M&B, Ry, Denmark) were used for rat brain membrane preparation. The animals were sacrificed by cervical dislocation, brains were removed, placed on ice, and *corpi striati* were dissected. The tissue was homogenized for 5-10 s in 100 volumes of ice-cold 0.32M sucrose using a motor driven glass/Teflon homogenizer. The homogenate was centrifuged at 1000 x g for 10 min (4°C), and the resulting supernatant was centrifuged at 27,000 x g for 50 min. The membrane pellet was

resuspended in 2000 volumes of 50 mM Tris-HCl buffer (pH 8.5) containing 5 mM KCl and 0.1% bovine serum albumin (BSA) and used for binding experiments.

The HEK293/hSK3 membrane suspension was thawed on the day of experiment, centrifuged for 10 min (27,000 x g) at 4°C and the final pellet was resuspended in ice-cold assay buffer (25-50 µg of protein/assay).

[¹²⁵I]Apamin binding conditions were as described previously (Finlayson et al., 2001). Briefly, binding assays were performed in a total volume of 2.2 ml consisting of 2.0 ml tissue suspension, 100 µl of test drug solution or buffer and 100 µl of [¹²⁵I]apamin (2.7-8.3 pM final concentrations). Samples were incubated for 90 min at 2°C, and binding was terminated by rapid filtration onto glass fiber filters (Whatman GF/C) presoaked 90 min with 0.25% polyethyleneimine (PEI), followed by three washes (5 ml) with ice-cold 50 mM Tris-HCl buffer (pH 8.5) containing 5 mM KCl. Non-specific binding was determined using unlabelled apamin (100 pM, final concentration). The radioactivity on the filters was determined using a Packard Cobra Auto-Gamma Counter. Compounds were tested at 8-12 concentrations ranging from 0.03 pM to 10 µM. All apamin solutions (in incubation buffer) contained 0.1% BSA to avoid adsorption to glass and plastic. All test drug stock solutions were prepared and diluted in 48% ethanol. Final ethanol concentration in the assay was 2%.

Electrophysiology on recombinant channels

Experiments were performed in the whole-cell, inside-out and outside-out configurations of the patch clamp technique. Cells seeded on cover slips were transferred to a 15 µl recording chamber grounded by an integrated AgCl pellet and superfused at 1 ml/min by gravity from an inlet tube connected to a 10 position solution exchanger (VICI, Houston, Texas, USA). Patch pipettes (1.8-2.3 MOhm) were pulled from borosilicate tubes (Modulohm, Copenhagen, Denmark) on a horizontal electrode puller (Zeitz Instruments, Augsburg, Germany) and positioned on the cells by an electronically controlled

micromanipulator (Eppendorf, Radiometer, Denmark). Experiments were controlled by an EPC-9 amplifier (HEKA, Lambrecht, Germany) connected to a Macintosh computer by an ITC-16 interface. Data were filtered at 3 kHz. In whole-cell experiments the series resistance was below 8 M Ω and 80% compensation was performed before application of each voltage-ramp or -step.

The extracellular solution for whole-cell experiments on SK1-SK3 and IK channels contained (in mM): 144 NaCl, 4 KCl, 0.1 CaCl₂, 3 MgCl₂ and 10 HEPES. pH was adjusted to 7.4 with NaOH. For experiments with inside-out or outside-out patches a high K⁺ solution (in mM: 154 KCl, 2 CaCl₂, 1 MgCl₂ and 10 HEPES with pH adjusted to 7.4 with KOH) was used on the extracellular side of the patch.

The intracellular solutions all contained 154 mM KCl and 10 mM HEPES as well as 10 mM EGTA or a combination of EGTA and NTA (10 mM in total). Concentrations of CaCl₂ and MgCl₂ needed to yield the desired free concentrations of Ca²⁺ (Mg²⁺ always 1 mM) were calculated by EqCal software (Cambridge, UK) and added. The free Ca²⁺ concentrations were controlled by a Ca²⁺-sensitive electrode (WPI, Sarasota, Florida, USA). For whole cell experiments a constant free concentration of 0.4 μ M was used in the pipette. This concentration was chosen to yield an intermediate activation of the SK channels. Excised patches were exposed to free [Ca²⁺]_i in the range from 0.01 to 10 μ M to cover the dynamic range of SK channel activation. All intracellular solutions were adjusted to pH 7.2 with concentrated HCl or KOH.

Slice preparations and electrophysiology

Transverse dorsal hippocampal slices (300 μ m thick) were prepared from adult C57BL/6J mice (20-60 days old) using a vibroslicer (Leica VT1000S), as previously described (Stocker et al., 1999). Throughout this procedure the brain hemispheres were maintained in oxygenated (95% O₂, 5% CO₂) artificial cerebrospinal fluid (ACSF) at ~4°C. The ACSF contained (in mM): 125 NaCl, 1.25 KCl, 2.5 CaCl₂, 1.5

MgCl₂, 1.25 KH₂PO₄, 24 NaHCO₃ and 16 glucose. The slices were subsequently incubated in a humidified interface chamber at room temperature (~24°C) for ≥ 1 hour.

Giga-seal whole-cell recordings were obtained from the somata of CA1 pyramidal cells using the 'blind' patch clamp technique (Blanton et al., 1989). Patch pipettes (4.0-6.5 MΩ) were pulled from borosilicate glass capillary tubes in a two-stage vertical puller (Narishige PP-830), and were filled with a pipette solution containing (in mM): 135 potassium methylsulphate, 10 KCl, 10 HEPES, 1 MgCl₂, 2 Na₂-ATP, 0.4 Na₃-GTP (pH 7.2-7.3 with KOH; osmolarity 280-295 mOsm). The pipette solution contained 50 μM 8-(4-chlorophenylthio)adenosine 3',5'-cyclic monophosphate (8CPT-cAMP) to inhibit sI_{AHP} (Stocker et al., 1999). Recordings were performed in a submersion chamber with a constant superfusion with oxygenated ACSF (2 ml/min) at room temperature. Once the whole-cell configuration had been established, the access resistance was regularly monitored and maintained at ≤ 25 MΩ for the duration of the experiment. No series resistance compensation and no corrections for liquid junction potentials were made.

Pyramidal cells were clamped at a membrane holding potential of -50 mV, and depolarized to +10 mV for 100 ms every 30 s in order to activate voltage-gated Ca²⁺ channels. The membrane potential was then stepped back to -50 mV where the I_{AHP} was visualized as a Ca²⁺-activated tail current. These experiments were conducted in the presence of 0.5 μM tetrodotoxin (TTX) and 1 mM tetraethylammonium (TEA) to block voltage-gated Na⁺ channels and some voltage-gated K⁺ channels. Data was generated and acquired using an EPC9 amplifier (HEKA, Germany) and the software Pulse (HEKA). Data was filtered at 1 kHz and sampled at 4 kHz.

Chemicals

[¹²⁵I]Apamin (2200 Ci/mmol) was purchased from PerkinElmer Life Sciences Inc. (Boston, MA). Apamin and TTX for slice electrophysiology were obtained from Latoxan (Rosans, France), d-tubocurarine (dTC)

from Fluka (Germany) and XE991 from Tocris (UK). Apamin and dTC for binding assays and experiments on cell lines, charybdotoxin (ChTX), TEA, clotrimazole (Clot), dequalinium chloride, Na₂ATP, Na₃GTP, dimethylsulfoxide (DMSO), 8CPT-cAMP were purchased from Sigma-Aldrich. Potassium methylsulphate was purchased from ICN Biomedicals Inc (Ohio, USA), and HEPES from Biomol (Hamburg, Germany). UCL 1684 (Campos Rosa et al., 2000) and NS309 (Jensen et al., 1999) were synthesized at NeuroSearch (Ballerup, Denmark). All other chemicals were purchased from regular commercial sources and were of the purest grade available.

For the electrophysiological experiments apamin, TTX, dTC, ChTX, and TEA was dissolved in the salt solutions used. Clot, dequalinium chloride, UCL 1684, NS309, and NS8593 were dissolved in DMSO and diluted at least 1000 times in the experimental solutions. The presence of 0.1 % DMSO had no effect on the currents recorded.

Calculations, fitting routines and statistics

IC₅₀ values were estimated from a non-linear regression fit to a Hill-type equation (**Eq. 1**):

$$B(C) = 1 - \frac{C^n}{IC_{50}^n + C^n} \quad (Eq.1)$$

B is the fraction of relative current in patch clamp experiments or specific binding in apamin binding experiments, C is the test concentration and *n* is the Hill coefficient.

K_i values for binding of test ligands were calculated from IC₅₀ values using the Cheng and Prusoff (1973) equation:

$$K_i = \frac{IC_{50}}{1 + C/K_d} \quad (Eq.2)$$

The K_d values determined for [125 I]apamin binding to striatal tissue and HEK293/hSK3 membranes were 4.1 and 4.0 pM, respectively.

K_d values for functional inhibition of SK channels were obtained by fitting SK current versus time data to **Eq.3** (Jenkinson, 1996):

$$B(C,t) = I - \frac{C}{K_d + C} \cdot \left(1 - e^{-(k_{off} + k_{on} \cdot C)t} \right) \quad (Eq.3)$$

where the dissociation constant K_d is defined as k_{off}/k_{on} (the dissociation (s^{-1}) - and association ($M^{-1}s^{-1}$) rate constants). For the equilibrium situation ($t \rightarrow \infty$) and for $n = 1$, **Eq.3** reduces to **Eq.1** (and thereby $IC_{50} = K_d$).

The potency of inhibition is throughout the paper given and discussed as the IC_{50} value when it is obtained by patch clamp equilibrium concentration-response experiments, as the K_d value when obtained by patch clamp kinetics experiments, and finally as the K_i value when obtained from displacement of radioactive apamin in equilibrium binding experiments.

Fitting routines were performed with the IGOR software (WaveMetrics, Lake Oswego, USA) using custom written macros, with Excel (Microsoft), Sigma plot, InStat and Prism (GraphPad Software Inc., San Diego, USA). Averaged data are given as means \pm SEM (standard error of the mean); statistical differences were determined by the students t test with $p = 0.05$ taken as level of significance.

Results

The novel compound NS8593 (Fig. 1A) was synthesized as part of a medicinal chemistry program (Sørensen et al, 2006). It is a chiral 2-aminobenzimidazole derivative without structural and physiochemical resemblance to any known SK channel blocker. In particular, NS8593 is a small (MW 263 g/mol), lipophilic compound (calculated logD = 3.9, pH 7.4) with basic properties, though without permanent positive charges.

Inhibition of recombinant SK3 channels by NS8593

The effect of NS8593 on typical whole-cell SK3 currents is illustrated in Fig. 1B. A prominent K⁺ current (Control; V_{rev} ~ -85 mV) was elicited by voltage-ramps (-120 mV to +30 mV) in a cell exposed to physiological salt gradients and perfused with a pipette solution buffered at 0.4 μM free Ca²⁺. Addition of 100 nM NS8593 reduced the current and shifted the V_{rev} towards more positive potentials, consistent with decreasing a K⁺ conductance. Superfusion with high concentrations of bicuculline methobromide (BMB; 100 μM) and apamin (30 nM) to the same cell completely blocked the current elicited at potentials more negative than -30 mV, demonstrating that it was mediated by SK channels. At more positive potentials a residual K⁺ current was observed in the presence of apamin and BMB due to activation of endogenous voltage-dependent K⁺ currents in HEK293 cells. The endogenous HEK293 K⁺ current was not significantly affected by NS8593 in the applied concentration range. The NS8593-induced inhibition of SK3 current was analyzed at -30 mV (arrow in Fig. 1B) and the entire time course of the experiment is depicted in Fig. 1C. Since BMB is an extremely fast and fully reversible blocker of SK channels, it was applied at the beginning of the experiment to identify the SK-mediated current. After washing out BMB, a reversible inhibition was induced by a three minutes application of NS8593 (100 nM). Finally, application of 30 nM apamin fully blocked the SK3 current.

Fig. 1D shows a concentration-response curve for the NS8593-induced reduction of the SK3-mediated current. An IC_{50} value of 91 nM was calculated by fitting to *Eq.1*. The Hill coefficient was 1.15, implying that the effect of NS8593 does not show cooperativity. Fig. 1D furthermore shows that full inhibition can be obtained.

The kinetics of the NS8593-induced inhibition was investigated from the same set of experiments as used for Fig. 1D. K_d values were calculated by fitting the time courses of the NS8593-induced decrease in current to *Eq.3*, and are plotted as a function of the compound concentration in Fig. 1E. Very similar K_d values are obtained when NS8593 is applied in the concentration range from 30 nM to 3 μ M. The data in Fig. 1D and Fig. 1E furthermore pinpoint that the mean of the K_d values (90 ± 8.0 nM, $n=33$), determined in this concentration range, is identical to the IC_{50} value obtained from the equilibrium concentration-response calculation (91 nM). Consequently, the kinetic approach was used in all subsequent experiments. The mean association- and dissociation rate constants for NS8593 was 1.4×10^5 $M^{-1}s^{-1}$ and 0.012 s^{-1} , respectively. For comparison, the k_{on} and k_{off} values obtained for apamin (applied at 0.3-1 nM) with the same method were 1.4×10^7 $M^{-1}s^{-1}$ and 0.0046 s^{-1} , respectively. The (S)-enantiomer of NS8593 also inhibited SK3 channels, although less potently than NS8593 ($K_d = 448 \pm 89$ nM, $n = 5$; data not shown). All data in Fig. 1 was obtained with the rat SK3 isoform but identical results were obtained with NS8593 and apamin on hSK3 channels (see Table 2). The affinity of NS8593 for rSK3 was also tested in symmetrical 154 mM K^+ solutions as used in the excised patch experiments (see later). Under these conditions the K_d value was slightly higher (169 ± 53 nM, $n=4$).

Selectivity of NS8593 towards other ion channels

The selectivity of NS8593 towards the other members of the SK/IK-family was tested. Fig. 2 shows a representative whole-cell experiment performed on hIK channels expressed in HEK293 cells. The experimental strategy is similar to the one used in Fig. 1. After stabilization of the whole-cell hIK current

upon Ca^{2+} -equilibration, the channel was blocked by addition of 100 nM charybdotoxin (ChTX), a reversible IK channel peptide blocker. After wash-out, 10 μM NS8593 was applied for four minutes, during which there was no associated decrease in current or change in the reversal potential. The experiment was terminated by addition of 1 μM clotrimazole (Clot). Thus, NS8593 discriminates between IK and SK types of voltage-independent, Ca^{2+} -activated K^+ channels. Table 1 further shows that NS8593 is inactive also on the voltage-dependent, large-conductance Ca^{2+} -activated K^+ channel (BK), and lists the effects of NS8593 on a number of other K^+ channels, as well as on voltage-dependent Na^+ and Ca^{2+} channels measured in the whole-cell patch clamp mode. NS8593 exhibits considerable selectivity for SK channels, but is not a specific inhibitor at concentrations exceeding 10 μM .

SK subtype selectivity

Apamin is the reference SK channel pore blocker, and it shows a characteristic SK channel subtype selectivity: $\text{SK2} = 0.074 \pm 0.01 \text{ nM}$ ($n=10$); $\text{SK3} = 0.33 \pm 0.05 \text{ nM}$ ($n=18$); $\text{SK1} = 2.9 \pm 0.3 \text{ nM}$ ($n=14$) based on K_d values from pooled whole-cell data (rat/human, 4 mM/150 mM extracellular K^+). For comparison, the SK subtype selectivity of NS8593 was explored in a series of experiments using excised multi-channel patches, where the channel activity is independent of the intracellular milieu. Since the recombinant rat SK1 channels do not readily express, the studies were performed on the human SK isoforms to avoid potential species-related differences. Symmetrical $[\text{K}^+]$ solutions were used in order to increase current amplitude and the holding potential was 0 mV, which largely inactivated the endogenous K_V channels. Fig. 3 shows the IV-relation for the three SK channel subtypes obtained from inside-out patches in the presence of 0.5 μM free Ca^{2+} before and after application of 3 μM NS8593 (left panels). There is no significant difference between the degree and kinetics of inhibition by NS8593 for all SK channel subtypes. The K_d -values (at -75 mV, in nM) were: 415 ± 101 (hSK1, $n=4$), 598 ± 51 (hSK2, $n=4$) and 726 ± 115 (hSK3, $n=7$). These values are not significantly different. Furthermore, no voltage-

dependence of NS8593-induced inhibition was detected for any of the subtypes (comparison of K_d values at -75 mV and at 75 mV, data not shown).

The K_d values obtained from inside-out patches on SK3 are higher than the corresponding values obtained in the whole-cell experiments at high potassium (726 nM vs. 169 nM). In the two configurations NS8593 is applied to the intracellular and extracellular side of the membrane, respectively. Furthermore, in whole-cell experiments the Ca^{2+} concentration cannot be accurately controlled, whereas the inside-out configuration isolates channel activity from cellular regulation including changes in Ca^{2+} concentration and channel phosphorylation. We therefore performed a series of experiments on inside-out and outside-out patches to test for a possible sidedness or a possible Ca^{2+} -dependence of the inhibitory action of NS8593 in the absence of ATP.

Ca^{2+} dependence of the NS8593-mediated inhibition

In Fig. 4A it is shown that NS8593 (3 μ M) induced a prominent reduction of the SK3-mediated current when applied to outside-out patches in the presence of 0.5 μ M free Ca^{2+} in the pipette as observed in inside-out patches. Apamin (100 nM) and BMB (200 μ M) were added as control of the patch configuration and to pharmacologically isolate the SK-mediated current. NS8593 was tested in the presence of different Ca^{2+} concentrations and Fig. 4B shows the average time courses of inhibition plotted for 0.5 and 10 μ M intracellular Ca^{2+} from inside-out (open circles) and outside-out (closed circles) experiments, respectively. The curves represent the best fit to **Eq. 3**. NS8593 (3 μ M) caused an almost full inhibition of the SK3-mediated current at 0.5 μ M Ca^{2+} , whereas the inhibition was substantially smaller in the presence of 10 μ M Ca^{2+} . This is further quantified in Fig. 4C that shows a plot of the calculated K_d values as a function of the intracellular $[Ca^{2+}]$. The inhibition by NS8593 decreased with increasing intracellular $[Ca^{2+}]$ (0.3 to 10 μ M), but was not dependent on the side of compound application. Using inside-out patches the K_d value increased from 0.47 ± 0.11 μ M (n=5) at 0.3 μ M Ca^{2+} to 14 ± 3.4 μ M (n=6) at 10 μ M Ca^{2+} . The corresponding values for outside-out patches were 0.70 ± 0.20 μ M (n=7) and

$6.6 \pm 1.5 \mu\text{M}$ ($n=6$). This shows that the affinity of NS8593 for SK channels is Ca^{2+} -dependent, and the most likely explanation for the higher affinity observed in the whole-cell experiments is that the actual intracellular free Ca^{2+} concentration near the Ca^{2+} binding site on calmodulin is substantially lower than the nominal buffered $0.4 \mu\text{M}$ in the whole-cell pipette. Extrapolating the K_d vs. $[\text{Ca}^{2+}]_i$ curves from the excised patches suggests that the local concentration in the whole-cell configuration is more likely to be $0.1\text{--}0.2 \mu\text{M}$.

The mechanism underlying the Ca^{2+} -dependence of inhibition by NS8593 was analyzed further in inside-out patches. In these experiments, the intracellular $[\text{Ca}^{2+}]$ was varied systematically in small steps in the range of $0.01 \mu\text{M}$ (closed channels) to $100 \mu\text{M}$ (maximally Ca^{2+} -activated channels) in the absence or in the presence of NS8593. Examples of ramp IV curves obtained at $0.3 \mu\text{M}$, $0.5 \mu\text{M}$, and $10 \mu\text{M}$ Ca^{2+} in the absence of NS8593 is shown in Fig. 5A. In Fig 5B the same Ca^{2+} concentrations were used but in the presence of $3 \mu\text{M}$ NS8593. The currents obtained in $0.3 \mu\text{M}$ and $0.5 \mu\text{M}$ Ca^{2+} were clearly reduced by NS8593, whereas the inhibition was more modest in $10 \mu\text{M}$ Ca^{2+} (the dashed control curve represents the current in the same patch obtained in $10 \mu\text{M}$ Ca^{2+} in the absence of NS8593).

Fig. 5C shows a summary of the effect of NS8593 on the full activation curve for Ca^{2+} . In the control situation, hSK3 channels were highly sensitive to Ca^{2+} with an EC_{50} value of $0.43 \mu\text{M}$ and a Hill coefficient of 5.6 ($n=18$). In the presence of $3 \mu\text{M}$ NS8593, the channels had a reduced Ca^{2+} -sensitivity with an EC_{50} of $1.6 \mu\text{M}$ and a Hill coefficient of 2.0 ($n=6$). The observed shift in the activation curve for Ca^{2+} implicates that the effect of NS8593 is pronounced at the low Ca^{2+} concentrations, whereas the inhibition is essentially abolished at $30 \mu\text{M}$ Ca^{2+} . It should be noted that very similar Ca^{2+} activation curves were obtained of hSK1- and hSK2-mediated currents and that the affinity for NS8593 was Ca^{2+} -dependent on these subtypes as well (data not shown).

The pronounced Ca^{2+} -dependence of the NS8593 induced inhibition may reflect that NS8593 binds to and stabilizes the SK channel in a closed state. To elucidate this possibility we conducted experiments as outlined in Fig. 5D. After establishment of the leak current in $0.01 \mu\text{M}$ $[\text{Ca}^{2+}]_i$ the fast and monophasic

response to 3 μM $[\text{Ca}^{2+}]_i$ was demonstrated. The channels were then closed by a 4 min superfusion with 0.01 μM $[\text{Ca}^{2+}]_i$ in the presence of 3 μM NS8593. The subsequent hSK3 activation by 3 μM $[\text{Ca}]_i$ was now drastically changed to a biphasic response, consisting of an initial fast component followed by a slow sigmoid phase approaching the current level of the unmodified channel within 5 min. This illustrates that a significant inhibition developed during the closed period and the slow phase is interpreted as Ca^{2+} displacement of NS8593 gradually reducing the inhibition to 15 %. After wash out of NS8593 the deactivation/activation procedure was repeated, showing that the monophasic, fast response to 3 μM Ca^{2+} was completely restored and that NS8593 applied after Ca^{2+} activation inhibited hSK3 by 17 % in good agreement with the results from Fig. 4C and 5C.

Apamin binding

In order to investigate whether NS8593 interacts with the apamin binding site, [^{125}I]apamin binding studies were performed. Fig. 6 shows displacement curves for apamin, UCL 1684, dequalinium and NS8593 on HEK293 cells expressing hSK3 (A) and on rat striatal membranes (B), which predominantly express the SK3 isoform (Sailer et al, 2004). Apamin, UCL 1684 and dequalinium all fully inhibited the specific [^{125}I]apamin binding with Hill coefficients close to 1, whereas NS8593 only caused a 30% reduction at the highest concentrations tested. The rank order of potency in both preparations was apamin, UCL 1684, dequalinium and NS8593 ($> 10 \mu\text{M}$). A summary of binding K_i values and patch clamp K_d values is given in Table 2.

Interactions of NS8593 and apamin with the positive modulator NS309

The apparent mirror-like action of the positive and negative modulators on the activation curve for Ca^{2+} (left and right shift, respectively), may suggest that NS8593 inhibits the SK channel gating by an interaction that shares the mechanism of action or even the physical binding site with the positive

modulators such as 1-EBIO and NS309. It was tested whether NS8593 was able to inhibit SK3 channels, which were fully activated by a high concentration of the positive modulator NS309, in the presence of a low concentration of intracellular Ca^{2+} (Fig. 7A). Initially, the inside-out patch was exposed to 0.3 μM Ca^{2+} , partially activating the SK3 channels, and subsequent superfusion with 3 μM NS8593 at this $[\text{Ca}^{2+}]$ gave the expected pronounced inhibition ($87 \pm 1\%$; $n=5$). After wash out of NS8593 and a short exposure to 0.01 μM Ca^{2+} , the channel was activated by a combination of 0.3 μM Ca^{2+} (as before) and 10 μM NS309. Under these conditions, the inhibition by NS8593 was profoundly reduced ($16 \pm 3\%$; $n=3$). After sequential wash out of both compounds and a brief exposure to 0.01 μM Ca^{2+} , the channels were fully activated with 10 μM Ca^{2+} (in the absence of NS309). In the presence of such high $[\text{Ca}^{2+}]$, NS8593 exerted only a weak inhibitory effect ($26 \pm 6\%$; $n=6$). The experiment was concluded with a repetition of the initial NS8593 application in the presence of 0.3 μM Ca^{2+} . Similar experiments were performed using outside-out patches. In the experiment shown in Fig. 7B profound inhibitions of the hSK3 current activated by 0.3 μM Ca^{2+} in the pipette solution were first obtained upon superfusion with BMB (100 μM) and subsequently with NS8593 (3 μM). The channels were then further activated by application of NS309 (10 μM) and, as observed with the inside-out experiments, this diminished the inhibition obtained by 3 μM NS8593 from $77 \pm 4.3\%$ ($n=7$) to $17 \pm 2.0\%$ ($n=7$). In contrast to this, the addition of 0.3 nM apamin in the continued presence of NS309 resulted in the same K_d value (0.26 ± 0.10 nM, $n=5$) as observed in whole-cell experiments without NS309 (see Table II) indicating that apamin-mediated inhibition of SK3 channels, in contrast to NS8593, is independent of full occupancy by NS309 at the positive modulator site.

Effect of NS8593 on the SK-mediated I_{AHP} in hippocampal slices

Apamin-sensitive SK channels mediate I_{AHP} , a voltage-independent, Ca^{2+} -activated K^+ current, in hippocampal pyramidal neurons (Stocker et al., 2004, Stocker et al., 1999). In whole-cell voltage clamp

recordings from mouse CA1 pyramidal neurons the tail current following a depolarizing step to 10 mV was only partly suppressed by apamin (50 nM; $42.9 \pm 12.1\%$ peak amplitude inhibition; $n = 7$; Fig. 8A and E). The current remaining after SK channel blockade (Fig. 8A, “Apamin” panel, and 8B, “dTC” panel) was not Ca^{2+} -dependent, as tested by applying a nominally Ca^{2+} free ACSF containing 5 mM Mg^{2+} ($n = 4$; data not shown). It was largely suppressed by higher concentrations of TEA (5 mM; inhibition of residual current amplitude: $74.0 \pm 9.7\%$; $n = 7$; $p < 0.01$; inhibition of residual current integral (charge transfer): $96.6 \pm 3.4\%$; $n = 7$; $p < 0.0001$; data not shown), and by the Kv7/KCNQ/M channel blocker XE991 (5 μM ; inhibition of residual current amplitude: $80.5 \pm 7.6\%$; $n = 4$; $p < 0.01$; inhibition of residual current integral (charge transfer): $90.4 \pm 5.9\%$; $n = 4$; $p < 0.001$; Fig. 8F). Given its pharmacological profile, this residual current is most likely I_M , a non-inactivating, voltage-dependent K^+ current that is mediated by KCNQ channels (Gu et al., 2005). We did not investigate this current component in further detail, and focused instead on I_{AHP} that we isolated by subtracting the apamin- or dTC-resistant current from current traces obtained before and after NS8593 application (see for example Fig. 8A and B, right panels), or by applying XE991 to block the I_M component (see for example Fig. 8C). Application of 10 μM NS8593 significantly reduced the total tail current by inhibiting I_{AHP} (I_{AHP} amplitude inhibition: $86.7 \pm 5.1\%$; $n = 6$; $p < 0.0001$; I_{AHP} charge transfer inhibition: $87.2 \pm 4.0\%$; $n = 6$; $p < 0.0001$; Fig. 8B, D, G). Subsequent application of the SK channel blocker d-tubocurarine (50 μM) had no further effect on the remaining current amplitude or charge transfer ($n = 6$; $p > 0.1$; Fig. 8B), indicating that 10 μM NS8593 had completely suppressed the SK-mediated I_{AHP} . This was further confirmed by experiments performed in the presence of XE991 (5 μM) to suppress I_M , whereby the residual I_{AHP} was fully inhibited by 10 μM NS8593 (I_{AHP} amplitude inhibition: $98.4 \pm 1.6\%$; $n = 3$; $p < 0.001$; I_{AHP} charge transfer inhibition: $100 \pm 0\%$; $n = 3$; $p < 0.0001$; Fig. 8C). Although the concentration used in this set of experiments is lower than the K_d values reported for Kv7 and Cav channels (Table 1), we were concerned that NS8593 might still produce slight effects on these

conductances at 10 μ M. We therefore performed a second set of experiments using a lower concentration of NS8593 (3 μ M). As shown in Fig. 8A, application of NS8593 (3 μ M) resulted in a significant reduction of the total tail current amplitude by $49.9 \pm 6.0\%$ and the corresponding charge transfer by $67.8 \pm 9.2\%$ ($n = 3$; $p < 0.02$ for both measures). Subsequent application of the specific SK channel blocker apamin (50 nM) resulted in a slight further reduction of the tail current amplitude ($p < 0.03$; $n = 3$), but with no significant effect on the residual charge transfer ($p > 0.1$; $n = 3$). NS8593 (3 μ M) suppressed the amplitude of the SK-mediated I_{AHP} , obtained by subtraction, by $84.7 \pm 1.4\%$ ($n = 3$; $p < 0.0003$; charge transfer inhibition: $85.2 \pm 1.3\%$, $n = 3$; $p < 0.0001$), as shown in Fig. 8A, right panel, and Fig. 8G. No significant difference was observed between the effect of 3 and 10 μ M NS8593 (Fig. 8G), suggesting that 3 μ M is a nearly saturating concentration. The compound was, however, not tested at lower concentrations, since the time course of inhibition in the slices was rather slow, as illustrated in Fig. 8D, where inhibition by 10 μ M NS8593 develops over 15-20 min. Control currents were therefore recorded in the presence of DMSO at the same final concentration used for the application of 10 μ M NS8593 (0.1%; Fig. 8D). DMSO had no significant effect on the amplitude and only a small effect on the charge transfer of the recorded currents (amplitude: $86.1 \pm 8.9\%$; $n = 4$; $p > 0.2$; charge transfer: $89.0 \pm 2.5\%$; $n = 4$; $p < 0.03$). Altogether, these data show that NS8593 targets and strongly suppresses the SK-mediated I_{AHP} in mouse hippocampal pyramidal neurons.

Discussion

In this study, we have identified and characterized a novel compound, (*R*)-*N*-(benzimidazol-2-yl)-1,2,3,4-tetrahydro-1-naphtylamine (NS8593), which is a potent and selective inhibitor of SK channels. In contrast to well established pore blockers, like apamin and d-tubocurarine, NS8593 acts as an inhibitory gating modifier, interacting at a site distinct from the apamin binding site in SK channels. The evidence for this conclusion can be summarized as follows: I) The potency of inhibition by NS8593 is strongly dependent on the intracellular $[Ca^{2+}]$. II) NS8593 causes a shift to the right of the Ca^{2+} activation curve, in analogy with the positive modulators, which cause a shift to the left. III) Closed channel inhibition can be reversed by high Ca^{2+} . IV) NS8593 does not displace $[^{125}I]$ apamin in the concentration range used to inhibit the SK currents in electrophysiological experiments. V) In contrast to apamin, NS8593 exerts no selectivity towards the SK channel subtypes. VI) Also in contrast to apamin, NS8593 is a weak inhibitor of NS309-modulated SK channels. VII) NS8593 is structurally distant from the known SK blockers, and it does not fit into a recently described pharmacophore model for the external blocker site (Dilly et al., 2005). VIII) NS8593 is the first inhibitory compound described, that can reach its high-affinity binding site from both the inside and the outside of the cell membrane. Furthermore, this study shows that the inhibition by NS8593 follows the Hill-Langmuir formalism closely, since the non-equilibrium kinetics were mono-exponential for both inhibition and wash out and the potency determined from the kinetic measurements ($K_d = k_{off}/k_{on}$) equaled the IC_{50} determined from the concentration-response experiments.

The tail current measured from mouse CA1 pyramidal neurons was shown to be the sum of two components, I_M and I_{AHP} being sensitive to XE991 and apamin/tubocurarine, respectively. The negative modulation by NS8593 was effective in inhibiting the SK-mediated I_{AHP} . The Ca^{2+} dependence of the NS8593 potency suggests that neuronal SK channels mediating the I_{AHP} are not exposed to saturating concentrations of intracellular Ca^{2+} following the depolarizing pulses used in this study. This is in good agreement with previous experiments, in which the positive modulators 1-EBIO (Pedarzani et al., 2001),

DC-EBIO and NS309 (Pedarzani et al., 2005) increased the apamin-sensitive I_{AHP} elicited by a similar depolarization protocol.

From an enzyme kinetics point of view, the effect of NS8593 on SK channels can be described as a reduction in the Ca^{2+} affinity occurring concomitantly with a reduced cooperativity of Ca^{2+} binding. This is very much in analogy with the activators (1-EBIO) which accordingly cause an increase in Ca^{2+} affinity and slightly increase cooperativity (Pedarzani et al., 2001). However, the nature of the molecular mechanisms mediating the observed inhibitory gating modulation of SK channels by NS8593 is unknown as is also the case for the positive modulators, although the C-terminal has been shown to be involved for 1-EBIO (Pedarzani et al., 2001). The present study, which furthermore demonstrates that high concentrations of NS309 (at low Ca^{2+}) can also prevent NS8593 inhibition, shows that a functional interaction exists between the action of positive and negative modulators, an interaction which does not exist between the positive modulators and apamin (see Fig. 7b). The simplest possibility is that positive and negative modulators share their binding site and that the functional interaction represents a direct competition between the two compounds. Such an interaction is well described for other ion channels such as the benzodiazepine site on GABA receptors, where agonists, inverse agonists as well as antagonists bind at the same site (for a review, see Sieghart et al., 1994). Another example is the dihydropyridine site on L-type Ca^{2+} channels, which binds both negative and positive modulators (Greenberg et al., 1984). If the positive and negative modulators of SK channels share the same site it is noteworthy that NS8593 shows a high degree of selectivity for SK channels towards the IK channel, whereas the known positive modulators 1-EBIO and NS309 are more potent on IK than on SK channels (Strøbæk et al., 2004). However, even though the general gating mechanism depending on constitutively bound calmodulin is shared between SK and IK, it may be important to pay attention to the observed smaller steepness of the IK Ca^{2+} activation curve relative to SK (Ishii et al., 1997). Most likely this significant physiological difference reflects a structural variation among the SK and IK subtypes, a difference that may be related to the distinct gating-based pharmacology observed here. Future studies on

the molecular mechanism may involve mutagenesis studies using SK/IK chimeras and/or mutated calmodulin analogues.

Apamin was known as a very potent neurotoxin even before recognition of its molecular target. Intracerebral ventricular (ICV) injections cause severe convulsions and seizures and the peptide also exerts CNS toxicity after systemic administration. However, at low non-convulsive doses, apamin has distinct behavioral effects, indicating a potential therapeutic value of blocking SK channels. Apamin increases the cognitive performance of mice in the Morris water maze and in the object recognition test (Stackman et al., 2002) as well as in the Y-maze (Deschaux and Bizot, 2005). SK channels have been shown to exert a postsynaptic feedback regulation of the NMDA receptor-mediated depolarization and Ca^{2+} influx in dendritic spines (Ngo-Anh et al., 2005). The augmented cognitive performance induced by apamin might therefore be linked to a facilitation of the induction of long term potentiation. Apamin also reduced immobility time in the forced swimming test (Galeotti et al., 1999), an acute model for behavioral despair and a routine assay for the evaluation of the antidepressant potential of new drugs. This effect may be linked to an increased or changed pattern of electrical activity of monoaminergic neurons, which all express the SK3 subtype (Stocker and Pedarzani 2000; Tacconi et al., 2001).

Despite these promising findings, however, apamin remains a very toxic compound and all behavioral testing occurs at doses close to or even overlapping with the adverse effects (van der Staay et al., 1999). The reason for the limited therapeutic window may be the high potency and specific SK subtype selectivity of apamin, favoring SK2 over SK3 and SK1 channels. However, it cannot be excluded that the mode of action (pore blocking rather than modulatory inhibition) may in itself contribute to the development of uncontrolled neuronal firing leading to seizures. The molecular mechanism of action is thought to be an important safety and efficacy parameter for several CNS acting drug classes, such as use-dependent Na_v blockers (for review, see Tayler and Narasimhan 1997) and glutamate receptor antagonists (for review, see Parsons 2001). An ion channel block without any feedback from the physiological activation process is generally less tolerable than competitive antagonism or allosteric modulation. Thus,

Ca²⁺-dependent, inhibitory gating modulation, as described here for NS8593, may be anticipated to be most effective at neurons with relatively low firing frequencies, but ineffective at neurons with sustained, high frequency firing. NS8593 may therefore be effective in subtly changing firing patterns (e.g. switch a dopaminergic neuron from pace-making to burst mode, see Waroux et al., 2005; Yi and Shepard, 2006), without eliciting widespread neuronal hyperexcitability. Since NS8593 is a small molecule that does not carry any permanent positive charges and permeates cell membranes, it is potentially a compound that readily crosses the blood brain barrier *in vivo*. A gating modifying, reversible SK channel inhibitor of this type - and in particular a compound, which exhibits SK subtype selectivity and further improved selectivity towards other ion channels - may help the elucidation of SK channels as possible therapeutic targets for the treatment of psychiatric and neurological diseases.

Acknowledgements

The authors thank Dr Martin Stocker for useful discussions, and Dr Gayle M. Passmore for advice on the use of XE991. We thank Helle D. Rasmussen and Tine Sparre for technical assistance with the synthesis of NS8593. Jette Sonne, Anne Stryhn Meincke and Vibeke Meyland-Smith are acknowledged for their assistance with patch clamp experiments and Susanne Kalf Hansen and Anne B. Fischer for running the apamin binding experiments.

References

- Blank T, Nijholt I, Kye MJ, and Spiess J (2004) Small conductance Ca^{2+} -activated K^{+} channels as targets of CNS drug development. *Curr Drug Targets CNS Neurol Disord* **3**:161-167
- Blanton MG, Lo Turco JJ, Kriegstein AR (1989) Endogenous neurotransmitter activates N-methyl-D-aspartate receptors on differentiating neurons in embryonic cortex. *J. Neurosci. Methods* **30**:203-210
- Bond CT, Maylie J, and Adelman JP (2005) SK channels in excitability, pacemaking and synaptic integration. *Curr. Opin. Neurobiol.* **15**:305-311
- Campos Rosa J, Galanakis D, Piergentili A, Bhandari K, Ganellin CR, Dunn PM, Jenkinson DH (2000) Synthesis, molecular modeling, and pharmacological testing of bis-quinolinium cyclophanes: potent, non-peptidic blockers of the apamin-sensitive Ca^{2+} -activated K^{+} channel. *J. Med. Chem.* **43**:420-431
- Castle NA, Haylett DG, Morgan JM, Jenkinson DH (1993) Dequalinium: a potent inhibitor of apamin-sensitive K^{+} channels in hepatocytes and of nicotinic responses in skeletal muscle. *Eur. J. Pharmacol.* **236**:201-207
- Cheng Y, and Prusoff WH (1973) Relationship between the inhibition constant (K_i) and the concentration of inhibitor which causes 50 per cent inhibition (IC_{50}) of an enzymatic reaction. *Biochem. Pharmacol.* **22**:3099-3108
- Chicchi GG, Gimenez-Gallego G, Ber E, Garcia ML, Winkquist R, Cascieri MA (1988) Purification and characterization of a unique, potent inhibitor of apamin binding from *Leiurus quinquestriatus hebraeus* venom. *J. Biol. Chem.* **263**:10192-10197

- Deschaux O, Bizot JC (2005) Apamin produces selective improvements of learning in rats. *Neurosci. Lett.* **386**:5-8
- Dilly S, Graulich A, Farce G, Seutin V, Liegeois JF, Chavatte P (2005) Identification of a pharmacophore of SK_{Ca} channel blockers. *J.Enz. Inhib. and Med. Chem.* **20**:517-523
- Faber ES, Delaney AJ, and Sah P (2005) SK channels regulate excitatory synaptic transmission and plasticity in the lateral amygdala. *Nat. Neurosci.* **8**:635-641
- Finlayson K, McLuckie J, Hern J, Aramori I, Olverman HJ, and Kelly JS (2001) Characterisation of [(125)I]-apamin binding sites in rat brain membranes with HEK293 cells transfected with SK channel subtypes. *Neuropharmacology* **41**:341-350
- Galeotti N, Ghelardini C, Caldari B, and Bartolini A (1999) Effect of potassium channel modulators in mouse forced swimming test. *Br. J. Pharmacol.* **126**:1653-1659
- Greenberg DA, Cooper EC, and Carpenter CL (1984) Calcium channel 'agonist' BAY K 8644 inhibits calcium antagonist binding to brain and PC12 cell membranes. *Brain Res.* **305**:365-368
- Gu N, Vervaeke K, Hu H, and Storm JF (2005) Kv7/KCNQ/M and HCN/h, but not KCa2/SK channels, contribute to the somatic medium after-hyperpolarization and excitability control in CA1 hippocampal pyramidal cells. *J. Physiol.* **566**:689-715
- Ishii TM, Maylie J, and Adelman JP (1997) Determinants of apamin and d-tubocurarine block in SK potassium channels. *J. Biol. Chem.* **272**:23195-23200
- Jenkinson DH (1996) Classical Approaches to the Study of Drug-Receptor Interactions, in *Textbook of Receptor Pharmacology*. (Foreman JC and and Johansen T eds.) pp 3-62. CRC Press Inc, Boca Reton.

- Jensen BS, Jørgensen TD, Ahring PK, Christophersen P, Strøbæk D, Teuber L, and Olesen SP (1999) NeuroSearch A/S, assignee. International patent application WO 00/33834
- Ji H, and Shepard PD (2006) SK Ca^{2+} -activated K^{+} channel ligands alter the firing pattern of dopamine-containing neurons in vivo. *Neuroscience* EPUB
- Kohler M, Hirschberg B, Bond CT, Kinzie JM, Marrion NV, Maylie J, and Adelman JP (1996) Small-conductance, calcium-activated potassium channels from mammalian brain *Science* **273**: 1709-1714
- Ngo-Anh TJ, Bloodgood BL, Lin M, Sabatini BL, Maylie J, and Adelman JP (2005) SK channels and NMDA receptors form a Ca^{2+} -mediated feedback loop in dendritic spines. *Nat. Neurosci.* **8**:642-649
- Liegeois JF, Mercier F, Graulich A, Graulich-Lorge F, Scuvee-Moreau J, and Seutin V (2003) Modulation of small conductance calcium-activated potassium (SK) channels: a new challenge in medicinal chemistry. *Curr. Med. Chem.* **10**:625-47
- Parsons CG (2001) NMDA receptors as targets for drug action in neuropathic pain. *Eur. J. Pharmacol.* **429**:71-78
- Pedarzani P, Mosbacher J, Rivard A, Cingolani LA, Oliver D, Stocker M, Adelman JP, and Fakler B (2001) Control of electrical activity in central neurons by modulating the gating of small conductance Ca^{2+} -activated K^{+} channels. *J. Biol. Chem.* **276**: 9762-9769
- Pedarzani P, D'hoedt D, Doorty KB, Wadsworth JD, Joseph JS, Jeyaseelan K, Kini RM, Gadre SV, Sapatnekar SM, Stocker M, and Strong PN (2002) Tamapin, a venom peptide from the Indian red scorpion (*Mesobuthus tamulus*) that targets small conductance Ca^{2+} -activated K^{+} channels and afterhyperpolarization currents in central neurons. *J. Biol. Chem.* **277**:46101-46109

- Pedarzani P, McCutcheon JE, Rogge G, Jensen BS, Christophersen P, Hougaard C, Strøbæk D, Stocker M (2005) Specific Enhancement of SK Channel Activity Selectively Potentiates the Afterhyperpolarizing Current IAHP and Modulates the Firing Properties of Hippocampal Pyramidal Neurons. *J. Biol. Chem.* **280**:41404-41411
- Sailer CA, Kaufmann WA, Marksteiner J, and Knaus HG (2004) Comparative immunohistochemical distribution of three small-conductance Ca^{2+} -activated potassium channel subunits, SK1, SK2, and SK3 in mouse brain. *Mol. Cell. Neurosci.* **26**:458-469
- Schrøder RL, Jespersen T, Christophersen P, Strøbæk D, Jensen BS, and Olesen SP (2001) KCNQ4 channel activation by BMS-204352 and retigabine. *Neuropharmacology* **40**: 888-898
- Seutin V, and Johnson SW (1999) Recent advances in the pharmacology of quaternary salts of bicuculline. *TIPS* **20**:268-270
- Shakkottai VR, Regaya I, Wulff H, Faijoun Z, Tomita H, Fathallah M, Cahalan MD, Gargus JJ, Sabatier JM, and Chandy KG (2001) Design and characterization of a highly selective peptide inhibitor of the small conductance calcium-activated K^{+} channel, SKCa2. *J. Biol. Chem.* **276**:43145-43151
- Sieghart W (1994) Pharmacology of benzodiazepine receptors: an update. *J. Psychiatry. Neurosci.* **19**:24-29
- Stackman RW, Hammond RS, Linardatos E, Gerlach A, Maylie J, Adelman JP, and Tzounopoulos T (2002) Small conductance Ca^{2+} -activated K^{+} channels modulate synaptic plasticity and memory encoding. *J. Neurosci.* **22**:10163-10171
- Stocker M, Krause M, and Pedarzani P (1999) An apamin-sensitive Ca^{2+} -activated K^{+} current in hippocampal pyramidal neurons. *Proc. Natl. Acad. Sci. U S A.* **96**:4662-4667

- Stocker M, and Pedarzani P (2000) Differential distribution of three Ca^{2+} -activated K^+ channel subunits, SK1, SK2, and SK3, in the adult rat central nervous system. *Mol. Cell. Neurosci.* **15**:476-493
- Stocker M (2004) Ca^{2+} -activated K^+ channels: molecular determinants and function of the SK family. *Nat. Rev. Neurosci.* **5**:758-770
- Stocker M, Hirzel K, D'hoedt D, and Pedarzani P (2004) Matching molecules to function: neuronal Ca^{2+} -activated K^+ channels and afterhyperpolarizations. *Toxicon* **43**:933-949
- Strøbæk D, Christophersen P, Holm NR, Moldt P, Ahring PK, Johansen TE, Olesen SP (1996) Modulation of the Ca^{2+} -dependent K^+ channel, hsk1, by the substituted diphenylurea NS 1608, paxilline and internal Ca^{2+} . *Neuropharmacology* **35**:903-914
- Strøbæk D, Teuber L, Jørgensen TD, Ahring PK, Kjær K, Hansen RS, Olesen SP, Christophersen P, and Skaaning-Jensen B (2004) Activation of human IK and SK Ca^{2+} -activated K^+ channels by NS309 (6,7-dichloro-1H-indole-2,3-dione 3-oxime). *Biochim. Biophys. Acta.* **1665**:1-5
- Syme CA, Gerlach AC, Singh AK, and Devor DC (2000) Pharmacological activation of cloned intermediate- and small-conductance Ca^{2+} -activated K^+ channels. *Am. J. Physiol. Cell. Physiol.* **278**:C570-581
- Sørensen US, Teuber L, Peters D, Strøbæk D, Johansen TH, Nielsen KS, and Christophersen P. NeuroSearch A/S, assignee. International patent application WO 2006/013210
- Tacconi S, Carletti R, Bunnemann B, Plumpton C, Merlo Pich E, and Terstappen GC (2001) Distribution of the messenger RNA for the small conductance calcium-activated

potassium channel SK3 in the adult rat brain and correlation with immunoreactivity.

Neuroscience **102**:209-215

Taylor CP, and Narasimhan LS (1997) Sodium channels and therapy of central nervous system diseases. *Adv. Pharmacol.* **39**: 47-98

van der Staay FJ, Fanelli RJ, Blokland A, Schmidt BH (1999) Behavioral effects of apamin, a selective inhibitor of the SK(Ca)-channel, in mice and rats. *Neurosci. Biobehav. Rev.* **23**:1087-2110

Waroux O, Massotte L, Alleva L, Graulich A, Thomas E, Liégeois JF, Scuvée-Moreau J, and Seutin V (2005) SK channels control the firing pattern of midbrain dopaminergic neurons *in vivo*. *Eur. J. Neurosci.* **22**:3111-3121

Xia XM, Fakler B, Rivard A, Wayman G, Johnson-Pais T, Keen JE, Ishii T, Hirschberg B, Bond CT, Lutsenko S, Maylie J, and Adelman JP (1998) Mechanism of calcium gating in small-conductance calcium-activated potassium channels. *Nature* **395**:503-507

Footnotes

*) This work was supported by the Medical Research Council (CEG to P.P.; Ph.D. fellowship to R.T.)

Legends for Figures

Fig. 1. NS8593 inhibits recombinant SK3 channel activity

A, The chemical structure of NS8593. **B**, Whole-cell current-voltage (I/V) relationships, measured in HEK293 cells stably expressing rSK3, upon application of 200 ms-long voltage ramps (-120 to +30 mV), elicited every 5 s from a holding potential of -90 mV. The experiment was conducted with 4 mM K⁺ in the extracellular solution and a pipette solution with a free Ca²⁺ concentration of 0.4 μM. I/V relationships were measured in the absence of compound (Control) and in the presence of bicuculline methobromide (BMB; 100 μM), Apamin (30 nM) or NS8593 (100 nM). The arrow indicates the point of analysis. **C**, SK3 current at -30 mV obtained from voltage ramps (panel **B**) as a function of time. The cell was exposed to BMB (100 μM), NS8593 (100 nM), and Apamin (30 nM) as indicated by bars. **D**, Concentration-response relationship for NS8593 obtained from experiments conducted as in panel **C**. Residual current in the presence of NS8593 is depicted as a function of NS8593 concentration. The solid line is the fit of the data to the Hill equation, yielding an IC₅₀ value of 91 nM and a Hill coefficient of 1.15. Each data point is the mean ± SEM of 5 to 12 experiments. **E**, Dissociation constant, K_d, as a function of the NS8593 concentration. K_d values, estimated from the kinetic fit described in the Methods, were obtained from the same experiments used for the IC₅₀ estimate summarized in panel **D**. The dotted line symbolizes a mean K_d of 90 nM.

Fig. 2. NS8593 does not affect recombinant IK channel activity

A, Whole-cell current-voltage (I/V) relationship, measured in HEK293 cells stably expressing hIK. Voltage protocol and solutions were as described in Fig. 1A. I/V relationships were measured under control conditions and after applications of charybdotoxin (ChTX, 100 nM), NS8593 (10 μM, n = 12), or clotrimazole (Clot, 1 μM). **B**, Whole-cell IK current at -30 mV plotted as a function of time. ChTX (100 nM), NS8593 (10 μM), and Clot (1 μM) were applied as indicated by bars.

Fig. 3. NS8593 inhibits SK1, SK2 and SK3 channels equipotently

Currents measured from inside-out patches obtained from HEK293 cells stably expressing hSK1 (**A**), hSK2 (**B**) or hSK3 (**C**) upon application of 200 ms-long voltage ramps (-80 to +80 mV) elicited every 5 s from a holding potential of 0 mV. Each I/V plot (left panels) shows a control trace and a trace obtained in the presence of 3 μ M NS8593 (applied to the bath/intracellular solution). The free $[Ca^{2+}]$ in the bath/intracellular solution was 0.5 μ M in all experiments. In the right panels, the current at -75 mV is depicted as a function of time. NS8593 (3 μ M) was applied as indicated by bars. The K_d values for NS8593-induced inhibition are (mean \pm SEM, in nM): 415 ± 101 (SK1, $n = 4$), 598 ± 51 (SK2, $n = 4$) and 726 ± 115 (SK3, $n = 7$).

Fig. 4. NS8593 inhibits SK3 channel activity equally well when applied to the intra- or the extracellular side of the membrane

A, Current at -75 mV measured from an outside-out patch obtained from a HEK293 cell stably expressing hSK3. The currents were obtained from 200 ms-long voltage ramps (-80 to +80 mV) elicited every 5 s from a holding potential of 0 mV. $[Ca^{2+}]_i$ was 0.5 μ M and NS8593 (3 μ M), Apamin (100 nM), and bicuculline methobromide (BMB, 200 μ M) were applied to the extracellular/bath solution as indicated by bars. **B**, Time-courses of the NS8593-induced inhibition of SK3 current at a $[Ca^{2+}]_i$ of 0.5 μ M (left panels) and 10 μ M (right panels). The two upper panels are derived from inside-out (IO) experiments (\circ), whereas the two lower panels are from experiments performed in the outside-out configuration (\bullet). Currents were normalized with respect to the steady-state current before NS8593 (3 μ M) application. Data points are mean \pm SEM of 4-9 experiments. **C**, K_d as a function of $[Ca^{2+}]_i$ measured from inside-out (\circ) and outside-out (\bullet) patches. Outside-out and inside-out experiments are labeled **OO** and **IO**, respectively.

Fig. 5. NS8593 inhibits SK3 channel activity in a Ca^{2+} -dependent manner

A, Current-voltage (I/V) relationship measured from inside-out patches obtained from HEK293 cells stably expressing hSK3. The currents were obtained from 200 ms-long voltage ramps (-80 to +80 mV) elicited every 5 s from a holding potential of 0 mV. The panel to the left shows an inside-out patch exposed to a $[\text{Ca}^{2+}]_i$ of 0.3, 0.5 or 10 μM as indicated. **B**, 3 μM NS8593 was present in the solutions containing 0.3, 0.5 or 10 μM free Ca^{2+} , except for the dashed trace, which was obtained in 10 μM Ca^{2+} after NS8593 wash out. **C**, Ca^{2+} concentration-response curves measured under control conditions or in the presence of 3 μM NS8593. The current at -75 mV was measured from inside-out patches exposed to increasing $[\text{Ca}^{2+}]_i$ either in the absence (\circ) or in the presence of 3 μM NS8593 (\bullet). Currents from individual patches were normalized with respect to the effect of 10 μM Ca^{2+} , which induces maximal SK3 activity. Data points are mean \pm SEM of 18 experiments under control conditions and 6 experiments in the presence of NS8593 (3 μM). The solid lines are the fit of data to the Hill equation, yielding an EC_{50} value for Ca^{2+} of 0.42 μM and a Hill coefficient of 5.6 under control conditions and of 1.6 μM and 2.0 in the presence of NS8593 (3 μM). **D**, Inhibition of the channels in the deactivated state. The current at -75 mV was measured from an inside-out patch exposed 0.01 and 3 μM $[\text{Ca}^{2+}]_i$ as indicated at the abscissa axis. NS8593 (3 μM) was present in the bath solutions as indicated by the bars.

Fig. 6. Apamin, UCL 1684, Dequalinium, but not NS8593, inhibit [¹²⁵I]apamin binding

Inhibition of [¹²⁵I]apamin binding to **A**, membranes from HEK293 cells stably expressing hSK3, and **B**, rat striatal membranes by apamin (●), UCL 1684 (○), dequalinium (■), and NS8593 (□). HEK293/hSK3 or striatal membranes were incubated with [¹²⁵I]apamin (2.7-8.3 pM) in 50 mM Tris-HCl buffer (pH 8.5) containing 5 mM KCl, 0.1% BSA and competing compounds. Binding was terminated after 90 min by filtration. Each data point represents the mean ± SEM for 3-4 experiments. Curve fitting was performed as described in data analysis. IC₅₀ values for HEK293/hSK3: apamin: 2.9 pM; UCL 1684: 950 pM; dequalinium: 190 nM; NS8593 > 10 μM; and for striatal membranes: apamin: 3.8 pM; UCL 1684: 270 pM; dequalinium: 290 nM; NS8593 > 10 μM.

Fig. 7. The NS8593-mediated inhibition of SK3 is diminished by the positive modulator NS309

A, Current at -75 mV measured from an inside-out patch obtained from a HEK293 cell stably expressing hSK3. The inside-out patch was exposed to a [Ca²⁺]_i of 0.01, 0.3 or 10 μM as indicated. At 0.3 μM Ca²⁺, 0.3 μM Ca²⁺ + 10 μM NS309 or 10 μM free Ca²⁺, 3 μM NS8593 was applied as indicated by bars. The K_d values for NS8593-induced inhibition were 0.30 μM at 0.3 μM Ca²⁺, 27 μM at 0.3 μM Ca²⁺ with 10 μM NS309, and 24 μM at 10 μM Ca²⁺. **B**, SK3 current from an outside-out patch exposed to 100 μM BMB and 3 μM NS8593 in the absence of NS309 and then 3 μM NS8593 and 0.3 nM apamin in the presence of 10 μM NS309 as indicated by the bars. The K_d values for NS8593-induced inhibition were 0.43 μM in the absence and 8.9 μM in the presence of NS309. The K_d value for apamin was 0.16 nM. The pipette solution contained 0.3 μM free Ca²⁺. In both **A** and **B** the currents were obtained from 200 ms-long voltage ramps (-80 to +80 mV) elicited every 5 s from a holding potential of 0 mV. Outside-out and inside-out experiments are labeled **OO** and **IO**, respectively.

Fig. 8. NS8593 inhibits the SK-mediated neuronal I_{AHP}

A, Tail currents measured in a mouse CA1 pyramidal neurons activated by 100 ms depolarizing pulses to 10 mV elicited every 30 s from a holding potential of -50 mV. The tail currents before and after application of 3 μ M NS8593 is shown in the two left panels and the combined inhibition by NS8593 and apamin (50 nM). Right panel: the SK-mediated component of the tail current, I_{AHP} , was obtained by subtracting the current trace obtained in the presence of apamin from the control and NS8593 traces. **B**, Tail currents obtained as in **A**, but with 10 μ M NS8593 and using d-tubocurarine (dTC, 50 μ M) as a reference SK blocker. Right panel: I_{AHP} was obtained by subtracting the current trace obtained in the presence of dTC from the control and NS8593 traces (see also **A**). **C**, Tail currents obtained as in **A**, but in the presence of the Kv7/KCNQ/M channel blocker XE991 (5 μ M, left panel). Further addition of 10 μ M NS8593 led to a full suppression of I_{AHP} (middle panel). The right panel shows superimposed traces obtained in the presence of XE991 before (I_{AHP}) and after (NS8593) the application of 10 μ M NS8593. Similar results were obtained in 3 cells. **D**, Time course showing the effect of 10 μ M NS8593 on the normalized amplitude of the total tail current (comprising the SK-mediated I_{AHP} and a Ca^{2+} -independent, TEA-sensitive component) (\circ , $n = 6$). Control data was recorded in the presence of 0.1% DMSO (\bullet , $n = 4$). The depolarizing step was applied every 30 s. 10 μ M NS8593 or 0.1% DMSO were applied at the time point indicated by the arrow. **E**, Bar diagram summarizing the effect of apamin (50 nM) on the total tail current. In 7 cells, apamin suppressed $42.9 \pm 12.1\%$ of the current peak amplitude and $55.1 \pm 9.9\%$ of the charge transfer, measured as the area underneath the outward current. **F**, Bar diagram summarizing the effect of XE991 (5 μ M) on the tail current elicited as described in **A** and remaining after the application of apamin (50 nM). In 4 cells, in the presence of apamin, XE991 suppressed $80.5 \pm 7.6\%$ of the residual current peak amplitude and $90.4 \pm 5.9\%$ of the charge transfer. **G**, Bar diagram summarizing the maximal effect of different concentrations of NS8593 (3 μ M, $n = 3$ and 10 μ M, $n = 6$) on the amplitude (black bars) and charge transfer (white bars) of the SK-mediated I_{AHP} obtained by subtraction (see **A** and **B**). Error bars are SEM.

Table 1

Effect of NS8593 on selected ion channels

NS8593 was tested in whole-cell experiments and K_d values were obtained from a fit to Eq. 3. Voltage ramp protocols were used for SK3, IK and BK channels, whereas standard voltage step protocols were used for the other channels listed. Recombinant channels were expressed in HEK293 cells and the native channels were measured in rat embryonic Dorsal Root Ganglion (eDRG) neurons

Ion channel	Result
<i>Recombinant</i>	
rSK3, K_d (μ M)	0.090 ± 0.008 (n=33)
hIK (10 μ M)	No effect (n=12)
hBK (10 μ M)	No effect (n=3)
hK _v 7.2+7.3, K_d (μ M)	18 ± 4.5 (n=6)
hERG (10 μ M)	No effect (n=5)
rNa _v 1.2, K_d (μ M)	39 ± 7.2 (n=5)
<i>Rat eDRG neurons</i>	
K _v , K_d (μ M)	27 ± 4.0 (n=4)
Na _v , K_d (μ M)	33 ± 7.6 (n=5)
Ca _v , K_d (μ M)	58 ± 6.2 (n=3)

Table 2

Inhibition of HEK293/hSK3 currents and of [¹²⁵I]apamin binding to HEK293/hSK3 and striatal membranes

K_d values calculated from whole-cell hSK3 measurements as shown in Fig. 1 and K_i values from binding experiments using rat striatal membranes and membranes from HEK293 cells stably expressing hSK3. All values shown are mean ± SEM from 3-7 experiments. In binding experiments the calculated Hill coefficients were in the range 0.88-1.24.

	Patch clamp, hSK3 K _d (nM)	Binding, hSK3 K _i (nM)	Binding, Striatum K _i (nM)
Apamin	0.23 ± 0.08	0.0018 ± 0.0004	0.0030 ± 0.0004
UCL 1684	1.8 ± 0.30	0.37 ± 0.03	0.17 ± 0.04
Dequalinium	136 ± 17	115 ± 25	156 ± 13
NS8593	69 ± 9	>10,000	>10,000

Figure 1

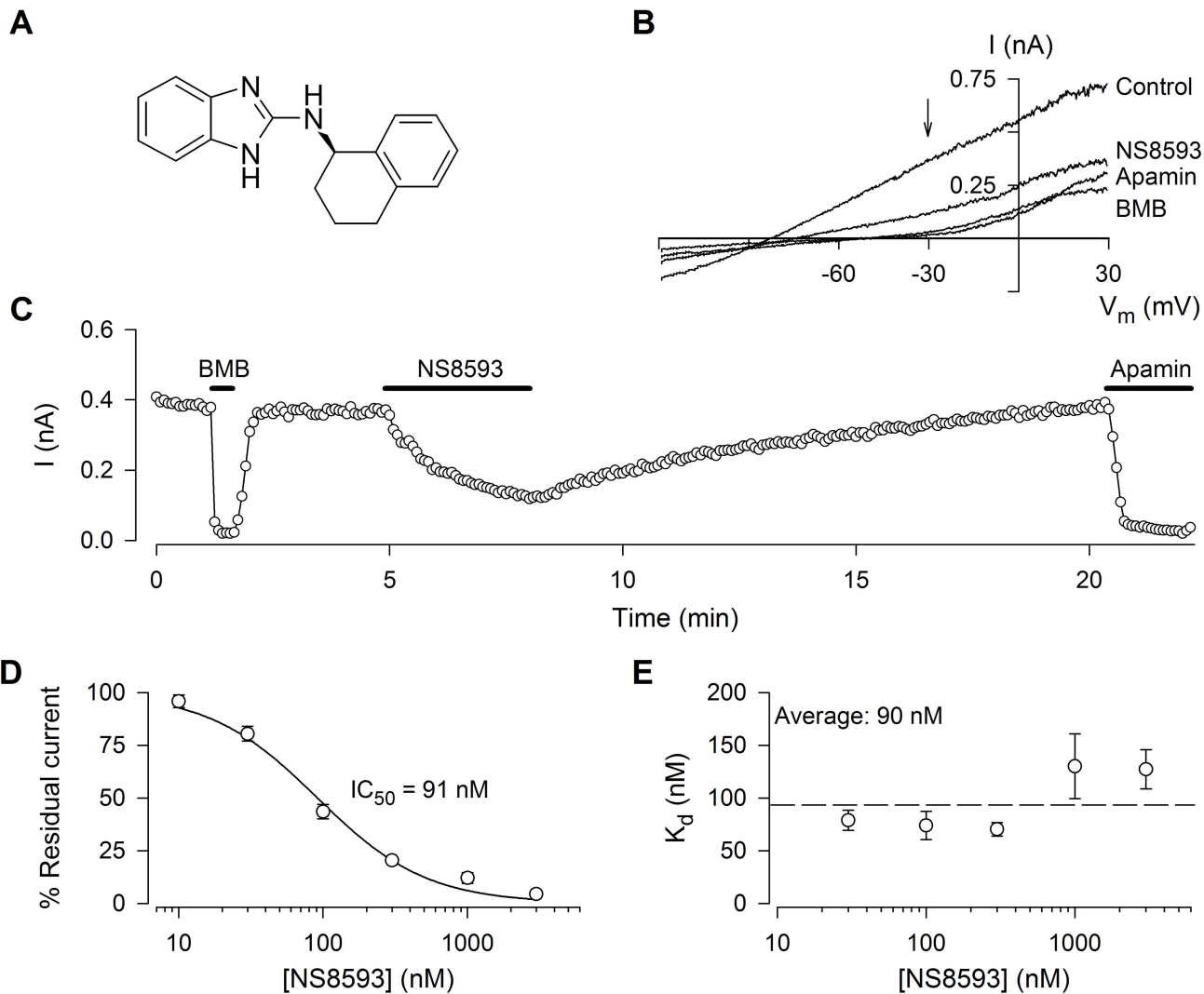
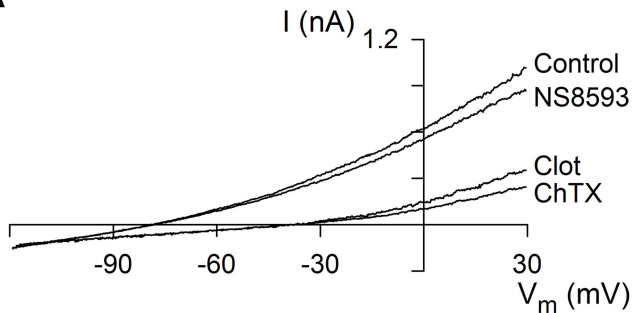


Figure 2

A



B

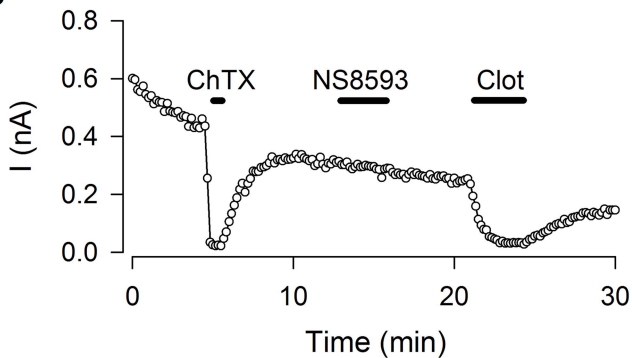


Figure 3

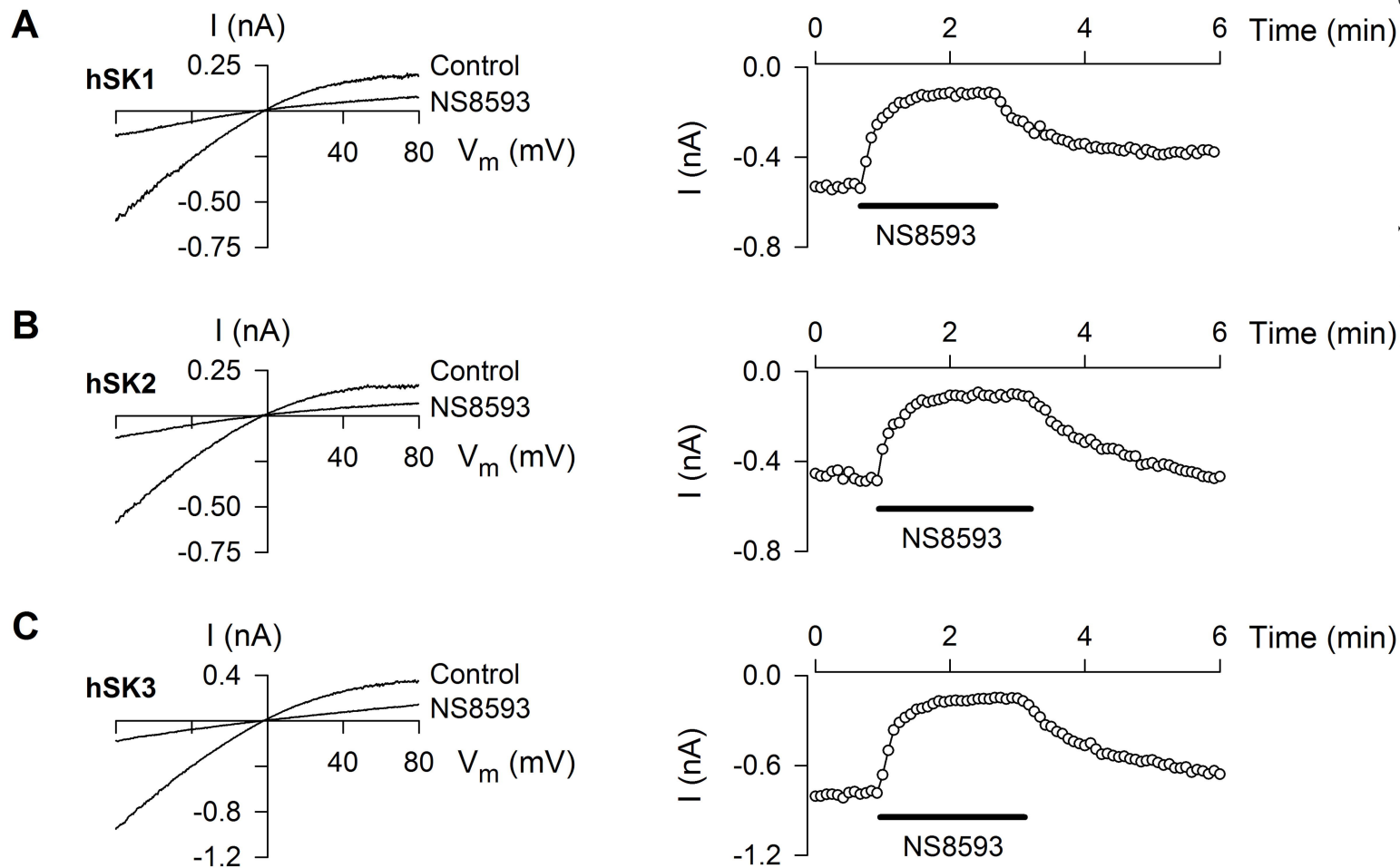
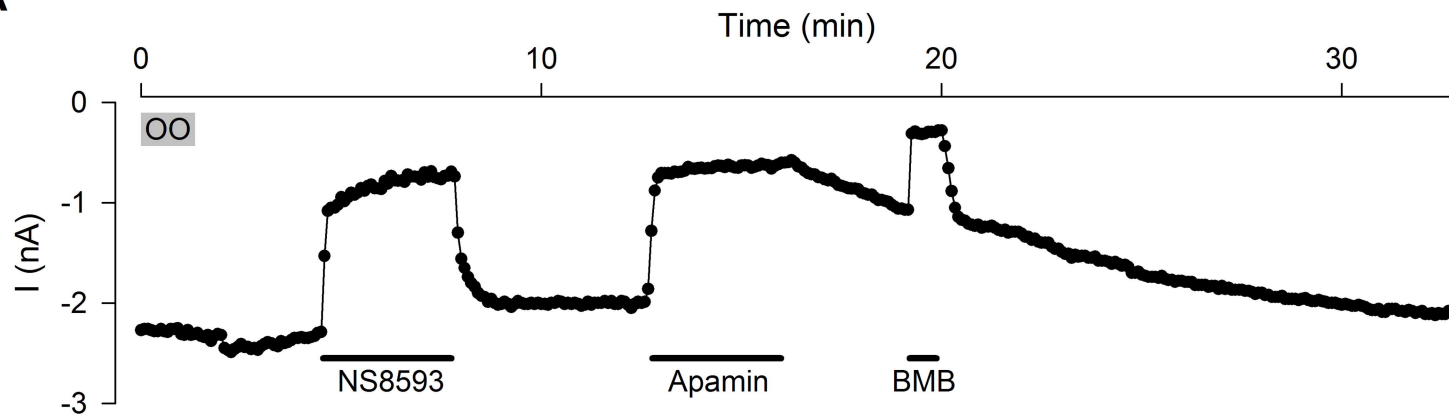
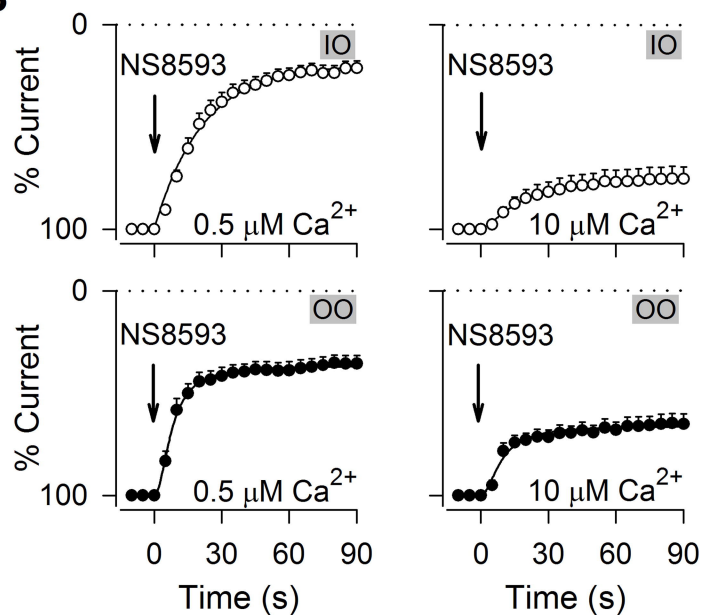


Figure 4

A



B



C

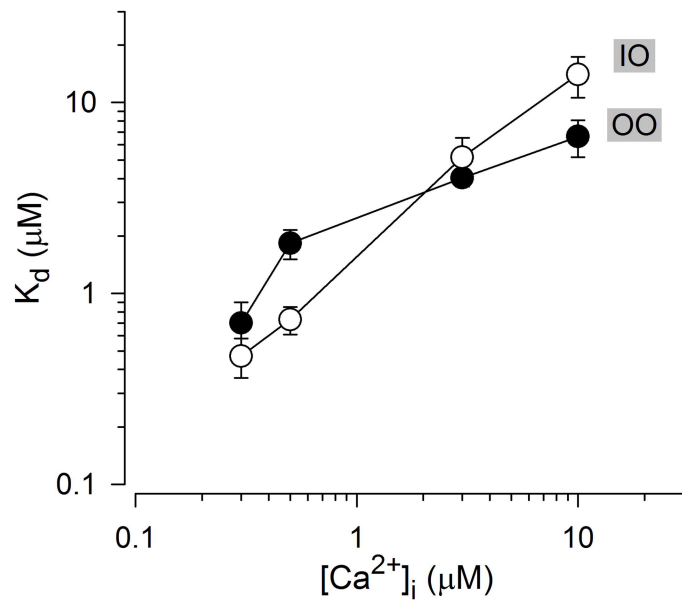


Figure 5

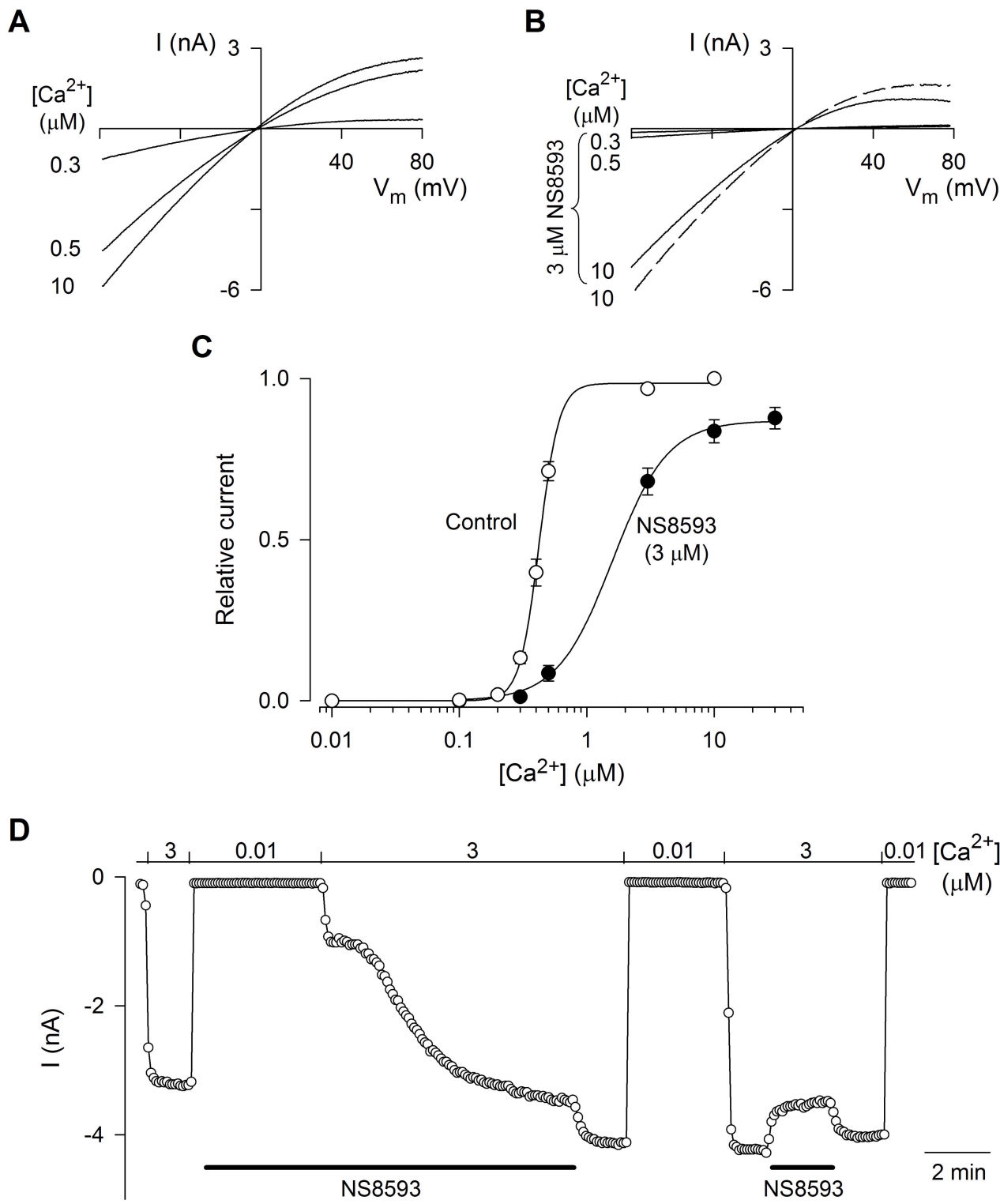


Figure 6

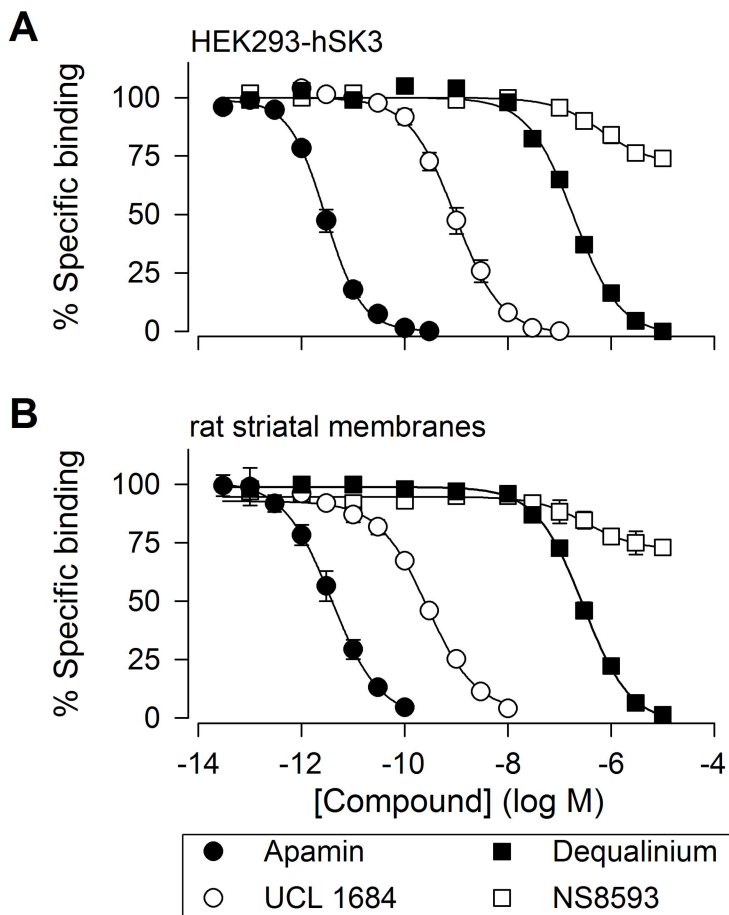
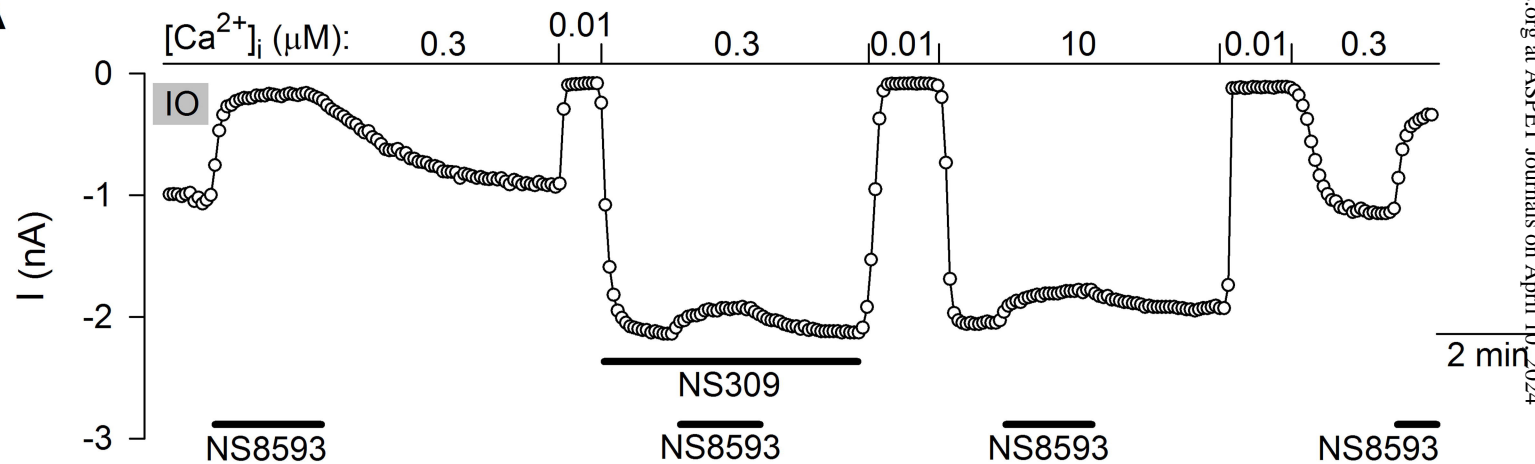


Figure 7

A



B

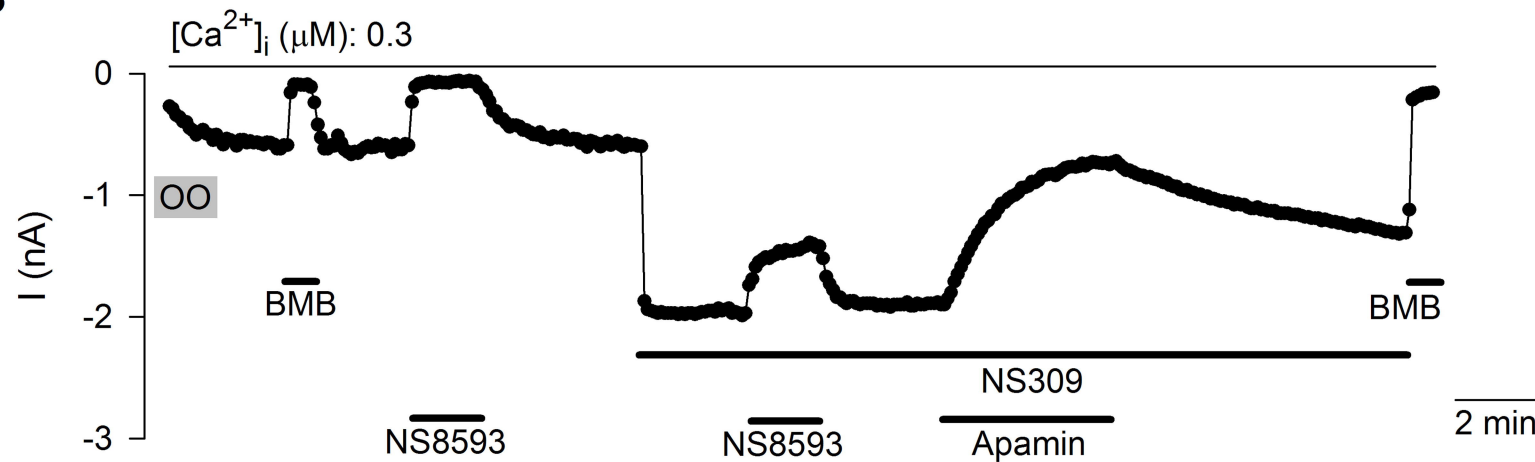
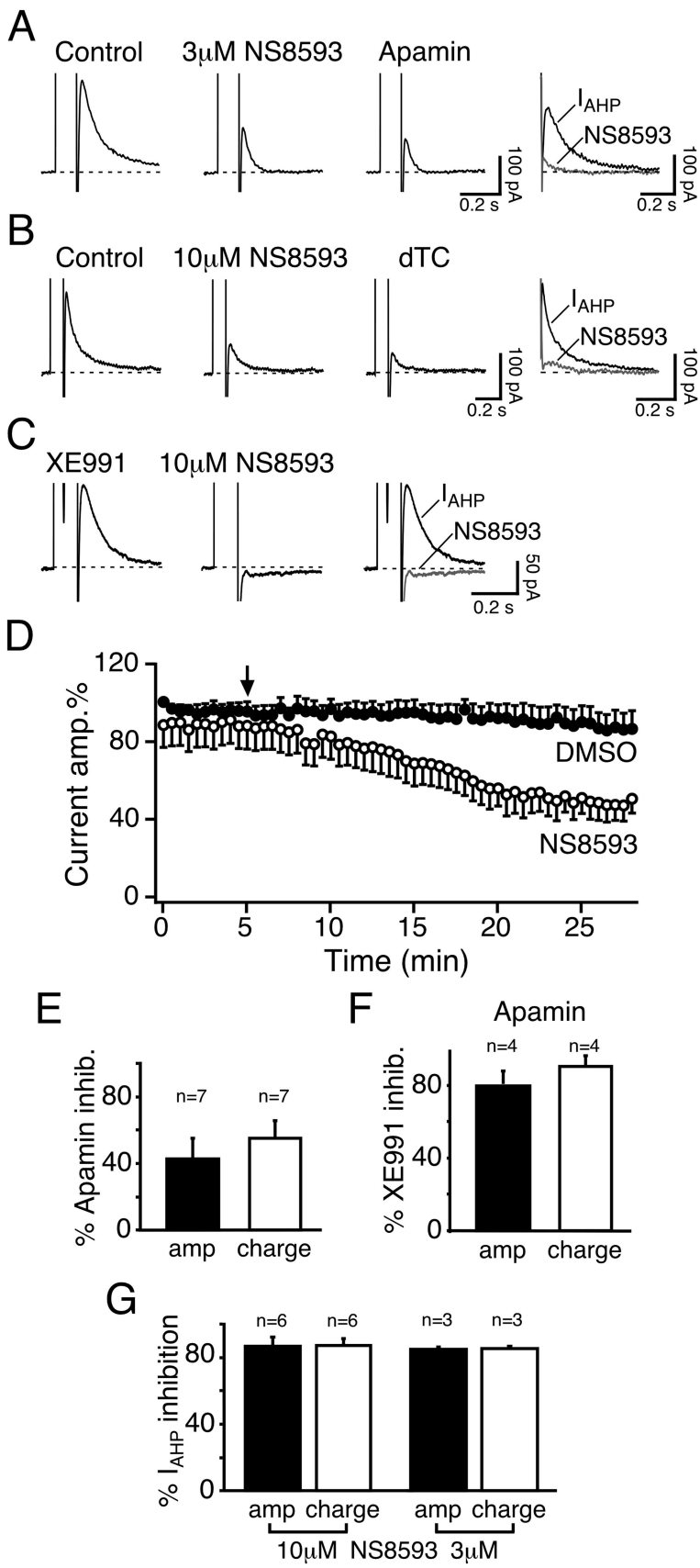


Figure 8



Scheme 1

